

UNCLASSIFIED

AD NUMBER

AD464731

NEW LIMITATION CHANGE

TO

**Approved for public release, distribution
unlimited**

FROM

**Distribution authorized to U.S. Gov't.
agencies and their contractors;
Administrative/Operational Use; APR 1965.
Other requests shall be referred to Air
Force Materials Lab., AFSC,
Wright-Patterson AFB, OH 45433.**

AUTHORITY

AFML ltr, 7 Dec 1972

THIS PAGE IS UNCLASSIFIED

16 19
ML TDR-64-21-Pt. 2

464731

6 ULTRASONIC WAVE PROPAGATION AND
INTERACTION IN SOLID MATERIALS

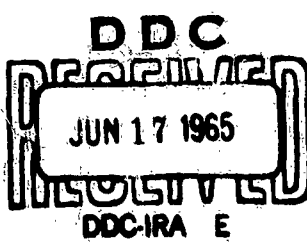
TECHNICAL DOCUMENTARY REPORT No. ML-TDR-64-21, PART II

9 Rept. For 28 Nov 63 - 28 Nov 64,

10 APR 1965,

AIR FORCE MATERIALS LABORATORY
RESEARCH AND TECHNOLOGY DIVISION
AIR FORCE SYSTEMS COMMAND
WRIGHT-PATTERSON AIR FORCE BASE, OHIO

16 Proj. 7360, Task 736002



15

Contract AF 33(657)11008,
5 Midwest Research Institute, Kansas City, Mo.
10 b by F. R. Rollins, Jr.

AD No.

FILE COPY

464731

NOTICES

When Government drawings, specifications, or other data are used for any purpose other than in connection with a definitely related Government procurement operation, the United States Government thereby incurs no responsibility nor any obligation whatsoever; and the fact that the Government may have formulated, furnished, or in any way supplied the said drawings, specifications, or other data, is not to be regarded by implication or otherwise as in any manner licensing the holder or any other person or corporation, or conveying any rights or permission to manufacture, use, or sell any patented invention that may in any way be related thereto.

Qualified requesters may obtain copies of this report from the Defense Documentation Center.

DDC release to CFSTI not authorized. The distribution of this report is limited because the report contains technology identifiable with items on the strategic embargo lists excluded from export or re-export under U. S. Export Control Act of 1949 (63 STAT. 7), as amended (50 U.S.C. App. 2020.2031), as implemented by AFR 400-10.

Copies of this report should not be returned to the Research and Technology Division unless return is required by security considerations, contractual obligations, or notice on a specific document.

FOREWORD

This report was prepared by Midwest Research Institute under USAF Contract No. AF 33(657)-11006. The contract was initiated under Project No. 7360, "The Chemistry and Physics of Materials," and Task No. 736002, "Non-destructive Methods." The work was administered under the AF Materials Laboratory, Research and Technology Division, Air Force Systems Command, with Mr. Harold Kamm acting as project engineer.

The period of work covered by this report is from 28 November 1963 to 28 November 1964.

The experimental work was largely conducted by Mr. F. R. Rollins, Jr., and Mr. P. Todd. Most of the theoretical work was performed by Mr. L. Taylor. Mr. Rollins served as project leader under the supervision of Mr. Gordon Gross, Head of the Physics Section, and Dr. Sheldon L. Levy, Director of the Mathematics and Physics Division.

ABSTRACT

Further exploration of ultrasonic beam interactions has been conducted and a review of the state-of-the-art is given. Improvement in the measurement of absolute intensities and an independent evaluation of the third-order elastic constants has permitted a fairly accurate comparison between theoretical predictions of intensity of interaction and experimental results. A four-beam interaction is also shown to be weaker than the previously observed three-beam interaction. A discussion is also directed toward the energy partition that occurs when ultrasonic beams impinge on a liquid-solid boundary. An ultrasonic goniometer is described for partial investigation of this energy partition. Experimental results are given for various metals and layered composites.

This technical documentary report has been reviewed and is approved.

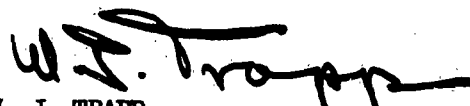

W. J. TRAPP
Chief, Strength and Dynamics Branch
Metals and Ceramics Division
Air Force Materials Laboratory

TABLE OF CONTENTS

	PAGE
I. INTRODUCTION	1
II. INTERACTION OF ULTRASONIC BEAMS	1
A. THEORY	1
B. EXPERIMENTAL	2
III. A REVIEW OF THE STATE-OF-THE-ART OF ULTRASONIC BEAM INTERACTION, ULTRASONIC BIREFRINGENCE, AND NONDESTRUCTIVE TESTING	9
IV. ENERGY PARTITION UPON REFLECTION AT A LIQUID-SOLID BOUNDARY . .	14
A. GENERAL	14
B. EXPERIMENTAL APPARATUS	17
C. RESULTS	19
D. PAPERS, PUBLICATIONS, AND MEETINGS	27
REFERENCES	28

ILLUSTRATIONS

FIGURE NO.	TITLE	PAGE
1	CIRCUIT ARRANGEMENT FOR MEASURING PULSED ULTRASONIC BEAM INTENSITY	4
2	THEORETICAL ENERGY PARTITION FOR A WATER-ALUMINUM BOUNDARY (AFTER MAYER (REF. 5))	15
3	SCHEMATIC OF APPARATUS FOR STUDYING REFLECTED BEAM AMPLITUDE VERSUS ANGLE OF INCIDENCE, α	18
4	PERCENTAGE OF INCIDENT ULTRASONIC ENERGY THAT IS REFLECTED VERSUS THE ANGLE OF INCIDENCE FOR 304 STAINLESS STEEL AND 6061-T6 ALUMINUM	20
5	AMPLITUDE OF REFLECTED SIGNAL VERSUS ANGLE OF INCIDENCE FOR (1) BARE ALUMINUM, AND ALUMINUM SUBSTRATES COATED WITH ACRYLIC RESIN PAINT HAVING THICKNESSES OF (2) 0.0005 IN., (3) 0.0011 IN., (4) 0.002 IN.	22
6	PER CENT OF INCIDENT AMPLITUDE VERSUS ANGLE OF INCIDENCE FOR BRASS AND LUCITE. TO COMPARE THE TWO CURVES, THE LUCITE AMPLITUDES SHOULD BE REDUCED BY A FACTOR OF 10	23
7	AMPLITUDE OF REFLECTED SIGNAL VERSUS ANGLE OF INCIDENCE FOR (A) 0.002 IN. THICK BRASS ON LUCITE, AND (B) 0.0042 IN. THICK BRASS ON LUCITE	25
8	EXPERIMENTAL CURVES FOR (A) 304 STAINLESS STEEL, (B) STAINLESS STEEL WITH 1/2 MIL THICK ELECTROPLATED COPPER, AND (C) COPPER	26

I. INTRODUCTION

This report describes work performed during the second year of a contract under which ultrasonic wave propagation and interaction effects in solid materials have been investigated. This work has been directed toward phenomena which will facilitate or improve current ultrasonic nondestructive test techniques or permit development of new techniques. Part I (Ref. 1) of this report describes early investigations of the nonlinear interaction between ultrasonic beams in solid media. These phenomena provide the research worker with a new technique of investigating subsurface properties and have important implications to a variety of NDT problems.

The study of interaction phenomena has continued during this report period. Additional confirmation between theoretical and experimental results was obtained and applications of the phenomena in the area of non-destructive testing were investigated. Most of the applications considered involved immersion techniques for coupling one or more of the ultrasonic beams into the specimen of interest. Since interaction intensity is often a variable of interest in such applications, considerable effort was directed toward the accurate determination of beam intensity and how the intensity varied across a liquid-solid interface as a function of incidence angle. An investigation of the latter effect revealed some rather interesting results which are applicable to NDT examination of coating and thin-film characteristics. The experimental arrangement for studying such characteristics and some of the results are discussed in subsequent sections of this report.

II. INTERACTION OF ULTRASONIC BEAMS

A. Theory

Some theoretical aspects of ultrasonic beam interaction were further investigated during the early part of this report period. However, since most of the theoretical treatment has appeared in previous reports and the entire theory is now in the open literature (Refs. 2 and 3) we will not go into the details of this work. It is sufficient to say that the various theoretical approaches used to study the interaction problem are now in excellent agreement with each other and in good agreement with experimental results (Ref. 4).

Manuscript released by the author January 1965 for publication as an RTD Technical Documentary Report.

Childress and Hambrick (Ref. 5) have recently published a theoretical paper in which they analyze the interaction problem using a wave packet formalism. The approach is an interesting one which in many respects closely approximates our experimental conditions. Order of magnitude agreement seems to exist between experimental results and either theoretical treatment. A more careful evaluation of experimental pulse shape, beam widths, etc., is necessary to completely evaluate the relative accuracy of the two approaches.

B. Experimental

At the conclusion of the last report period there were still certain basic aspects of the interaction phenomenon that needed further experimental investigation. These included measurement of absolute beam intensities, comparison of theoretical and experimental intensities, and an investigation of four-beam interactions. Our effort in each of these three areas is discussed below.

1. Measurement of Absolute Beam Intensities

The correlation of interaction beam intensities with theoretical predictions and the subsequent utilization of interaction phenomena to evaluate third-order elastic constants are very dependent on the experimental measurement of ultrasonic intensities. Estimates of intensity can be achieved from knowledge of the transducer voltage and piezoelectric equivalent circuit theory. Unless the experimenter has an independent scheme for evaluating the quality of the bond between transducer and specimen, the calculated intensity may be in serious error. There are a number of techniques for direct measurement of ultrasonic beam intensities but the majority of these techniques requires continuous excitation of the transducer rather than pulsed excitation, or certain requirements are placed on the specimen that are not easily met in interaction experiments. However, Alers and Fleury (Ref. 6) have suggested a pulsed technique of measuring the ultrasonic strain amplitude in a solid where variations in transducer bond are evaluated by comparing the decay in voltage oscillations across the transducer in the bonded and unbonded condition. Considerable effort was directed toward the utilization of this technique in interaction experiments but a number of difficulties were encountered. These will be discussed along with a description of the technique.

The experimental arrangement as used by us is shown in Figure 1. The low impedance output (93Ω) of the Arenberg pulsed generator was terminated with the primary winding of an air core transformer, the secondary of which is the inductance of a tuned tank that includes a tuning capacitance and the quartz transducer. The rf voltage across the tank is measured using an oscilloscope with an extremely high impedance input. The measurement of strain amplitude using this arrangement is based on the assumption that under pulsed conditions, the acoustic energy radiated will equal the electrical energy input if other losses are minimized such that (Ref. 6)

$$\frac{1}{2} \rho c^3 \epsilon_0^2 A = V^2/R \quad (1)$$

where ρ is the specimen density, c is the velocity of sound in the specimen, ϵ_0 is the strain amplitude, A is the active area of the transducer, V is the voltage applied to the transducer, and R is the electrical resistance associated with acoustic radiation into the test material. If ideal bonding is assumed, the value of R can be calculated using the expression

$$R = \frac{Z}{4\beta^2} \quad (2)$$

where Z is defined as $\rho c A$ and β is the transformation factor (Ref. 7) for the transducer. Since the impedance due to specimen loading as seen by the transducer is modified by the presence of the coupling bond between the transducer and specimen, the technique suggested by Alers and Fleury is directed toward the actual measurement of R rather than its mere calculation.

The measurement procedure involves excitation of the tank circuit with a short pulse of rf energy from the pulsed generator. If the tank is of sufficiently high Q , it will continue to "ring" for a considerable time after the driving pulse has stopped. These voltage oscillations ultimately decay at a rate that reflects the energy dissipation in the circuit. The measured rate of decay can be used to calculate the effective parallel impedance across the tank circuit from the expression:

$$R_P = \frac{\omega^2 L}{2} \left[\frac{t_1 - t_2}{\ln(A_1/A_2)} \right] \quad (3)$$

where A_1 is the amplitude of the decaying signal at t_1 and A_2 is the amplitude at t_2 .

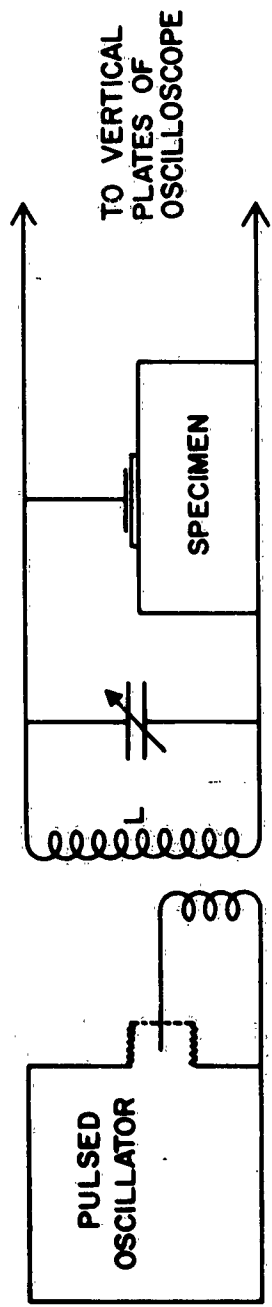


Figure 1 - Circuit Arrangement for Measuring Pulsed Ultrasonic Beam Intensity

L is the inductance in the tank circuit and ω is the angular frequency. R_p is first evaluated with the transducer oscillating freely in air, i.e., without any energy coupled into the specimen. This measurement provides an indication of nonacoustic losses in the circuit. The measurement is then repeated with the transducer bonded to the specimen and the resultant value of R_p' is assumed to be a parallel combination of R_p and the effective resistance, R , representing the acoustic energy loss from the transducer. The value of R can then be calculated from the two experimentally determined values of R_p and R_p' ; thus expression (1) becomes

$$\frac{1}{2} \rho c^3 e^2 A = \frac{V^2 (R_p - R_p')}{R_p R_p'} \quad (4)$$

There are several experimental conditions which must be met when the above technique is used. The technique is applicable to pulsed systems, and the measurement of the decaying voltage oscillations must be performed in the interval after the driving voltage goes to zero and before any echoes return to the transducer. Accuracy of the measurements is very dependent on a relatively high Q of the tank circuit. The voltage oscillations across a low Q tank will decay almost as rapidly as the driving pulse making it very difficult to evaluate R .

The experimental arrangement illustrated in Figure 1 was easily set up and initial results were encouraging. However, a more thorough examination of the data revealed a number of discrepancies which needed attention. Repeated measurements on the same crystal-bond-load arrangement yielded a rather widely divergent set of values for R . One of the main sources of this divergence was traced to a nonexponential decay of the voltage oscillations. The variations were sometimes subtle changes in decay rate with increasing time but it was often a more severe problem with obvious fluctuations superimposed on the exponential decay.

The more severe problem was largely eliminated by giving closer attention to accurate termination of the generator. A fairly satisfactory arrangement was accomplished by placing a 100Ω resistor in parallel with the primary transformer winding. Other termination resistances were used in an attempt to further improve results but very little improvement was accomplished. Incidentally, the addition of the resistor had a noticeable effect on the Q of the tank, and thus on the values of both R_p and R_p' . This result indicates that a fair amount of energy is reflected back into the "primary" section of the transformer.

After elimination of the more severe fluctuations, the subtle deviations from exponential decay were still a source of considerable scatter in our results. The origin of this nonexponential decay was not in the transducer, as was initially believed, because the effect was still present even when the transducer itself was completely removed from the circuit.

The above problem was never completely eliminated but it could be minimized through extremely careful tuning of the generator and the tank circuit. Our more consistent data still contained scatter of 20 - 30 per cent on the same bond. Although this error is greater than desired, it is an improvement over a straight calculation of intensity assuming ideal bonding.

2. Comparison of Theoretical and Experimental Intensity of Interaction

It has often been mentioned in previous reports that a direct and meaningful comparison of experimental and theoretical beam interaction results was impossible until the third-order elastic constants were known for one of the materials on which we have experimental results. Mr. R. T. Smith of Imperial College, London, has recently developed accurate velocity measuring techniques (Ref. 8) to evaluate third-order constants and he was kind enough to determine these constants for the specific magnesium samples used in our experiments. The Murnaghan constants, as determined by Smith, are given in Table I. The Murnaghan constants are, of course, very simply related (Ref. 8) to the Goldberg constants used in our theoretical treatment (Ref. 2) of the interaction phenomena. The Goldberg constants, as calculated from Smith's data, are therefore also shown in Table I.

TABLE I

THIRD-ORDER MODULI OF MAGNESIUM TOOL PLATE AS MEASURED BY SMITH

Murnaghan Notation (dynes/cm ²)			Goldberg Notation (dynes/cm ²)		
<u>l</u>	<u>m</u>	<u>n</u>	<u>A</u>	<u>B</u>	<u>C</u>
-9.01x10 ¹¹	-14.16x10 ¹¹	-26.2x10 ¹¹	-26.2x10 ¹¹	-1.06x10 ¹¹	-7.95x10 ¹¹

The above third-order elastic constants for magnesium have been used to calculate the expected third-beam displacement amplitudes in a variety of interaction cases. The agreement with experimental results is quite good

considering the difficulty of getting experimental values of ultrasonic beam intensities. Table II gives some of the more pertinent parameters for two typical interaction experiments together with values of X_3 , the third-beam displacement amplitude calculated according to Jones and Kobett (Ref. 2), and X_3' , the value determined experimentally using the techniques discussed in the preceding section.

TABLE II
COMPARISON OF THEORETICAL AND EXPERIMENTAL VALUES OF X_3
IN MAGNESIUM TOOLING PLATE

Interaction Case	$L+T \longrightarrow L(\omega_1+\omega_2)$	$T+T \longrightarrow L(\omega_1+\omega_2)$
Frequency ω_1	5 Mc/S	5 Mc/S
Frequency ω_2	8 Mc/S	5 Mc/S
Displacement Amplitude X_1	3.35×10^{-7} cm.	11.1×10^{-7} cm.
Displacement Amplitude X_2	4.80×10^{-7} cm.	11.1×10^{-7} cm.
Calculated Value X_3	3.93×10^{-11} cm.	8.0×10^{-10} cm.
Measured Value X_3'	7.7×10^{-12} cm.	6.7×10^{-11} cm.

Where comparisons were made, the measured values of X_3 were always less than the theoretical values. However, absolute values were usually within an order of magnitude of each other. Part of the error can be explained by the fact that attenuation of the ultrasonic beams is ignored in the theoretical calculations. Dissipation, of course, does reduce the measured values through attenuation of both the primary and scattered beams. Attenuation in magnesium is relatively low, but a reasonable correction of one-half to one-third should be applied to the values of X_3 shown in Table II. The resulting agreement between X_3 and X_3' is better than we might have expected. The Jones and Kobett theory, therefore, certainly appears to provide adequate predictions relative to the intensity of nonlinear interactions in isotropic solids.

3. Four-Beam Interactions

The generation and detection of a third ultrasonic beam as a result of two primary beams interacting in nonlinear solids is well established; but, for frequencies in the low megacycle range, the interaction is relatively weak. It was shown in the preceding section that the generated beam is typically 60 - 80 db. weaker than the primary beams. For ultimate application of the interaction phenomenon to such things as nondestructive measurements, etc., it is desirable to increase the intensity of the generated beam.

One proposed method of increasing the intensity of the generated beam involved the intersection of three beams rather than two. It is true that the resultant strain in the region of intersection would be greater than when only two beams intersect (assuming equal amplitude for all beams), but there are theoretical arguments that can be made suggesting that such an interaction will, in fact, be weaker than that represented by the intersection of two beams. Let us use the terminology of quantum mechanics to describe these two types of interaction, i.e., four-phonon or three-phonon interactions. The number refers to the total number of phonons (or beams in our case) taking part in the interaction.

It can be easily shown (Ref. 2) that the three-phonon interaction is primarily due to those terms in the elastic energy expression that are cubic in the particle displacements. The four-phonon interaction arises from the terms that are quartic in displacement. Quantitative expressions for the "intensity" of four-phonon interactions are quite laborious to derive. These expressions contain terms that involve the so-called fourth-order elastic constants. These constants have never been measured and we have little theoretical intuition about their magnitude. It is, however, generally conceded that the four-phonon interaction should be considerably weaker than the three-phonon interaction. Nevertheless, considering our success in studying the three-phonon interaction, it seemed appropriate that some effort should be directed toward an experimental examination of the four-phonon process.

It may be recalled that the conditions of resonance that had to be met in three-phonon interactions were in reality the conditions necessary to conserve energy and momentum. These conditions were in fact unique for a given material and combination of three phonons. We find, however, that for the four-phonon interaction a particular combination of waves may interact in a variety of ways and still conserve energy and momentum.

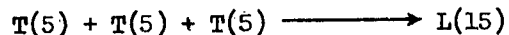
Let us consider the following four-phonon interaction:

$$T(\omega_1) + T(\omega_2) + T(\omega_3) \longrightarrow L(\omega_1 + \omega_2 + \omega_3) .$$

It is obvious that energy is conserved in this interaction. Momentum will be conserved if $\bar{k}_1 + \bar{k}_2 + \bar{k}_3 = \bar{k}_4$ where \bar{k}_i is the wave vector of the i^{th} beam. Conservation of momentum, however, can be achieved with \bar{k}_1 , \bar{k}_2 , \bar{k}_3 , and \bar{k}_4 having many different directions. It should be pointed out that two of the primary phonons may intersect at the correct angle for resonant three-phonon interaction. The resultant sum-frequency phonon ($\omega_1 + \omega_2$) could then interact with the ω_3 phonon at the correct angle to provide resonance for another three-phonon interaction, producing the final phonon of frequency

$(\omega_1 + \omega_2 + \omega_3)$. It is possible, although usually less probable, that the three primary phonons interact at angles that permit conservation in a direct transition to the final phonon without conservation to intermediate states.

A possible four-beam interaction was studied using two distinct geometries. The exact interaction selected was the following:



The specimen material was polycrystalline magnésium. The experiment was first set up such that two of the three primary beams intersected at the appropriate angle to produce the resonant generation of a 10-mc. longitudinal beam. The third transverse beam was incident at the correct angle to further satisfy conservation laws and thus theoretically generate a 15-mc. longitudinal beam. In this experiment, the 10-mc. beam was easily detected but the 15-mc. beam was undetectable. The peak-to-peak voltage applied to all of the 5-mc. transducers was 2,200 v. The voltage generated by the 10-mc. transducer was approximately 2 v. The noise level in our receiver system was such that we should have been able to detect a 15-mc. signal of about 0.002 v. Thus, if a 15-mc. beam was generated, its intensity was more than 60 db. below that of the 10-mc. beam. This is not too surprising since the 10-mc. beam itself was about 60 db. weaker than the 5-mc. beams.

In the second attempt to observe the 15-mc. beam, the three 5-mc. beams were intersected at angles which satisfied the conservation laws for the over-all interaction, but not for any intermediate interactions. Results were again negative.

The experiment described above is of considerable interest and value even though negative results were obtained. It confirms some of the generally accepted ideas about probability of four-phonon interactions and suggests that this is not a suitable technique for getting stronger ultrasonic beams from the interaction phenomenon.

III. A REVIEW OF THE STATE-OF-THE-ART OF ULTRASONIC BEAM INTERACTION, ULTRASONIC BIREFRINGENCE, AND NONDESTRUCTIVE TESTING

The experimental observation of interaction between ultrasonic beams in solid media was first reported by the author (Refs. 9 and 10) almost two years ago. Since that time, an intensive study of the interaction phenomena

has been conducted. The experimental program has confirmed many of the theoretical predictions and revealed many unknown aspects of the interaction geometry. In addition, we have gained a much better understanding of the nonlinear elastic properties of solid materials.

It seems appropriate at this point in our investigation to critically review the interaction phase, with particular emphasis on its limitations and applications in the area of nondestructive testing.

In this regard, it should be mentioned again that the interaction of ultrasonic beams in metals or other opaque specimens is something of a technological "breakthrough" in that it provides a technique of isolating a relatively small volume element (volume of interaction) within a much larger specimen, and, thus, making a three-dimensional analysis of certain subsurface properties.

Let us, therefore, examine the interaction process in the light of our current theoretical and experimental information, and critically analyze its potential in the field of nondestructive testing. It should be emphasized that our theoretical approach to the interaction problem was based on a completely isotropic medium and that the experimental effort to date has all been performed in material that is very nearly isotropic; at least, on a macroscopic basis. The effect of severe deviations from isotropic conditions will be discussed later.

Experimental observations of the interaction are normally carried out by intersecting two pulsed beams at the "resonant" angle and then detecting the third beam that is generated in the volume of interaction (Ref. 4). The third beam, of course, has a frequency ($\omega_1 + \omega_2$) and propagation vector ($\mathbf{k}_1 + \mathbf{k}_2$) where the subscripts refer to characteristics of the two primary beams. The criticality of the angular relationships between the three ultrasonic beams has been investigated and found to increase with frequency. In other words, at the higher frequencies, the interaction intensity will fall off very rapidly as the angle between the two primary beams is varied on either side of resonance. At lower frequencies, the intensity varies less rapidly with the angular variations. What then is the possibility of using the angulation characteristics of the interaction to nondestructively monitor variations in certain material properties? This is a difficult question to answer in general terms but some observations can be made. In materials that exhibit relatively weak attenuation at frequencies above 25 Mc., the angle of maximum interaction can be determined to an accuracy of better than 1/2 degree. Even much better results are possible in the 50 - 100 Mc. range but attenuation in most polycrystalline materials is so severe at these frequencies that interaction effects are difficult to observe.

Some idea of the magnitude of the property variations that would produce a change of 1/2 degree in the angle of maximum interaction can be obtained by examining the theoretical expressions that define the angle of resonance (Ref. 2). For example, the expression for the interaction of a longitudinal and a transverse beam to produce a sum-frequency longitudinal beam is shown below:

$$\cos \varphi = c + [a(c^2 - 1)/2c] ,$$

where φ is the angle for maximum interaction between two beams of frequency, ω_1 and ω_2 , the constant a is defined as the ratio ω_2/ω_1 , and $c = c_t/c_\ell$ where c_t and c_ℓ are the transverse and longitudinal velocities, respectively. Now consider a specimen in which the value of c varies somewhat within the material. Such variations might be a reflection of residual stresses, impurity concentrations, lack of uniform phase transformation, etc. From the above expression, one may easily determine how a small change in c affects φ . It is obvious that the exact value of $d\varphi/dc$ will depend on the frequency ratio, a , and the material constants as reflected in the velocity ratio, c . Nevertheless, several calculations for polycrystalline iron indicate that a variation in c values of 1 - 3 per cent is necessary to produce a change in φ equal to 0.5° . In other words, the ability to measure $\Delta\varphi$ values of 0.5° could be used to monitor $\Delta c/c$ values of 1 - 3 per cent. What does this mean -- relative to residual stress measurements? Using the shear wave interferometry technique to study stress induced anisotropy in several solids, we have previously shown (Ref. 12) that "yield-point" stresses usually produce $(\Delta V/V)$ values of less than 1 per cent. In this case, ΔV is defined as the velocity difference $(v_{11} - v_{1\perp})$ where one shear wave is polarized parallel and one is polarized perpendicular to the principal stress axis. The magnitude of $\Delta V/V$, however, should compare favorably with $\Delta c/c$ in the current study, if the variations are due to similar origin, i.e., stress effects.

From the above arguments it appears that, until further improvements are made in experimental techniques, beam angulation determinations are not sensitive enough to provide useful quantitative information about internal stresses. There are, however, other material properties that are more effective in producing changes in the elastic constants; thus, the determination of interaction angulation characteristics may be of value in nondestructively detecting untempered regions in tempered steel, regions of phase variation, concentrations of impurity due to nonuniform mixing, etc.

Besides the angular relationships discussed above, there are two additional characteristics of the interaction phenomena that could conceivably be utilized in nondestructive detection and measurement techniques. One is

the intensity of the third beam and the other is based on the polarization of shear waves involved in the interaction. Consider the intensity first. The intensity is dependent on so many material properties that it is difficult to imagine a technique in which one could unambiguously relate intensity fluctuations to variations of a specific property. The third-beam intensity is also dependent on the intensities of the two primary beams, as well as attenuation which may occur along the path length of any of the three beams. We see, therefore, that beam intensity measurements are probably the least rewarding from the standpoint of nondestructive testing except that rough estimates of third-order elastic constants can be gained from intensity measurements.

The polarization characteristics of interaction shear waves appear to be a more promising avenue of investigation. The feasibility of using the interaction phenomena to generate plane polarized shear waves has been amply demonstrated (Refs. 1 and 4). The interaction zone can be moved from point-to-point within a large sample, thus the polarization of the generated shear wave in propagating through various sections of the sample may be analyzed and related to material properties. The experimental details of such a feasibility study have been reported previously (Ref. 1), but certain limitations are inherent in the technique and should be understood.

In studying material properties that produce only very slight changes in ultrasonic velocities, there is often an advantage in using shear waves. This is particularly true if the velocity surfaces in the material under study are not completely spherical, i.e., when the velocity varies slightly with propagation direction. These differences are usually too small to detect with normal pulse echo velocity measurement techniques but they can be detected using interferometer techniques. The polarization of ultrasonic shear waves can often be controlled so that interferometric sensitivity can be achieved with a single beam. This technique has been described in previous reports (Refs. 11 and 12) and has been utilized in studying stress-induced anisotropy as well as other anisotropic conditions such as preferred orientation, etc. The so-called shear wave birefringence technique is capable of detecting anisotropic conditions where the fractional velocity difference, $\Delta V/V$, is even less than 10^{-4} . The exact sensitivity of the technique depends primarily on the geometry and attenuation of the material under study. Since the stress-induced anisotropy associated with yield-point stresses can produce $\Delta V/V$ values of $10^{-3} - 10^{-2}$, we see that shear wave birefringence is more than sensitive enough to accurately detect and, with appropriate calibration, measure stresses of only a fraction of yield stress magnitude. It is certainly true, however, that other sources of anisotropy are often present and, in fact, these anisotropies are usually larger than those due to stresses. In most polycrystalline metals, shear wave birefringence techniques yield information about the total anisotropy of the

media with the primary contributions coming from (1) preferred grain orientation and (2) stresses, in that order.

The normal pulse-echo technique of observing shear wave birefringence (Refs. 11 and 12) integrates the anisotropy over the total thickness of the specimen. It is easily seen that such a technique has serious limitations with respect to the measurement of residual stresses because surface stresses are usually balanced by subsurface stresses of opposite signs. The net effect would, therefore, usually give a "near zero" average stress. Preferred orientation on the other hand is usually more uniform and the birefringence will indicate an average anisotropy over the specimen thickness. The use of interaction techniques can alleviate the above problem somewhat by making it unnecessary to average the anisotropy over the entire thickness of the specimen. The shear wave can thus be originated at various points deep within the specimen and a comparison of total birefringence from adjacent regions can be used in analyzing the anisotropy at subsurface locations. The difficulty of separating stress effects from preferred orientation effects is still present, however.

One additional problem should be emphasized with respect to the use of interaction techniques along with shear wave birefringence as a means of studying structural variations within a material. Most of our experimental effort has been conducted in materials where the preferred orientation produces an anisotropy of tetragonal or orthorhombic symmetry. If a stress-induced anisotropy also exists, the principal axes are usually coincident with the orthogonal axes of the quasi crystal. For a shear wave to remain "pure mode" in such a medium, the propagation direction and the polarization direction must both coincide with one of the principal axes. Shear wave birefringence is normally observed by sending the shear wave along one principal axis with the initial polarization at 45° between the other two axes. The examination of an unknown specimen would seldom present such ideal conditions. In general, we find that ultrasonic propagation in directions that are not "principal" result in degradation of the pure mode configuration into one quasi-longitudinal component and two quasi-transverse components. The direction of maximum energy flow for each component generally will not coincide with the propagation vector or the principal axes. Analysis of particle-motion in these cases and correlation with the unknown anisotropy would be extremely difficult. The difficulty is compounded when the anisotropy due to preferred orientation does not have orthogonal symmetry.

From the above arguments it is clear that severe difficulties still exist in applying either the birefringence or interaction techniques to practical problems of residual stress measurements. These difficulties are not insurmountable, however, and in some applications they may not exist. For example, a change in residual stress will often occur without any attendant change in preferred orientation. If the change in residual stress is the variable

of primary interest in such cases, a combination of birefringence and interaction techniques (Ref. 1) would certainly be applicable to the problem. In addition, such techniques will undoubtedly find ultimate application in the simpler tasks of detecting regions of doubtful integrity (untempered areas in tempered steel), undesirable inhomogeneities, and even in flaw detection problems not easily solved by more established techniques.

IV. ENERGY PARTITION UPON REFLECTION AT A LIQUID-SOLID BOUNDARY

A. General

When an ultrasonic beam impinges on a liquid-solid boundary, the energy present in the incident beam may be partially or entirely reflected depending primarily on the angle of incidence. If only partial reflection occurs the "lost" energy is refracted into the solid as some combination of longitudinal, shear, and surface waves. The theoretical partition of energy between the reflected and refracted portions of the beam has received considerable interest recently (Refs. 13 and 14). This renewed interest in an old phenomenon has been at least partially due to high speed computers which make routine work of the long tedious calculations that evolve from the theory.

Figure 2 is taken from a paper by Mayer (Ref. 13) and illustrates the expected energy partition at a water-aluminum boundary when surface waves and absorption are not considered. Under these conditions the incident energy is partitioned only between the reflected (R) wave and the refracted longitudinal (L) and shear (S) waves. At normal incidence, a refracted shear wave does not exist so the energy is partitioned between the reflected and refracted longitudinal wave. The exact division at normal incidence is, of course, only dependent on the impedance mismatch at the boundary. As the angle of incidence is increased some energy goes into the refracted shear wave until the critical angle for the refracted longitudinal wave is reached. At this angle all of the energy is theoretically reflected back into the water. At higher angles the (S) wave receives a fairly large per cent of the incident energy until it also approaches its critical angle. In this somewhat simplified picture the incident energy would be totally reflected at all higher angles. When the possibility of surface waves is admitted to the theory a more complex situation exists but the major change occurs at an angle of incidence just beyond that which produces critical refraction of the shear wave. At this angle the energy in the reflected (R) wave dips again and the energy is converted into surface waves that propagate along the solid surface.

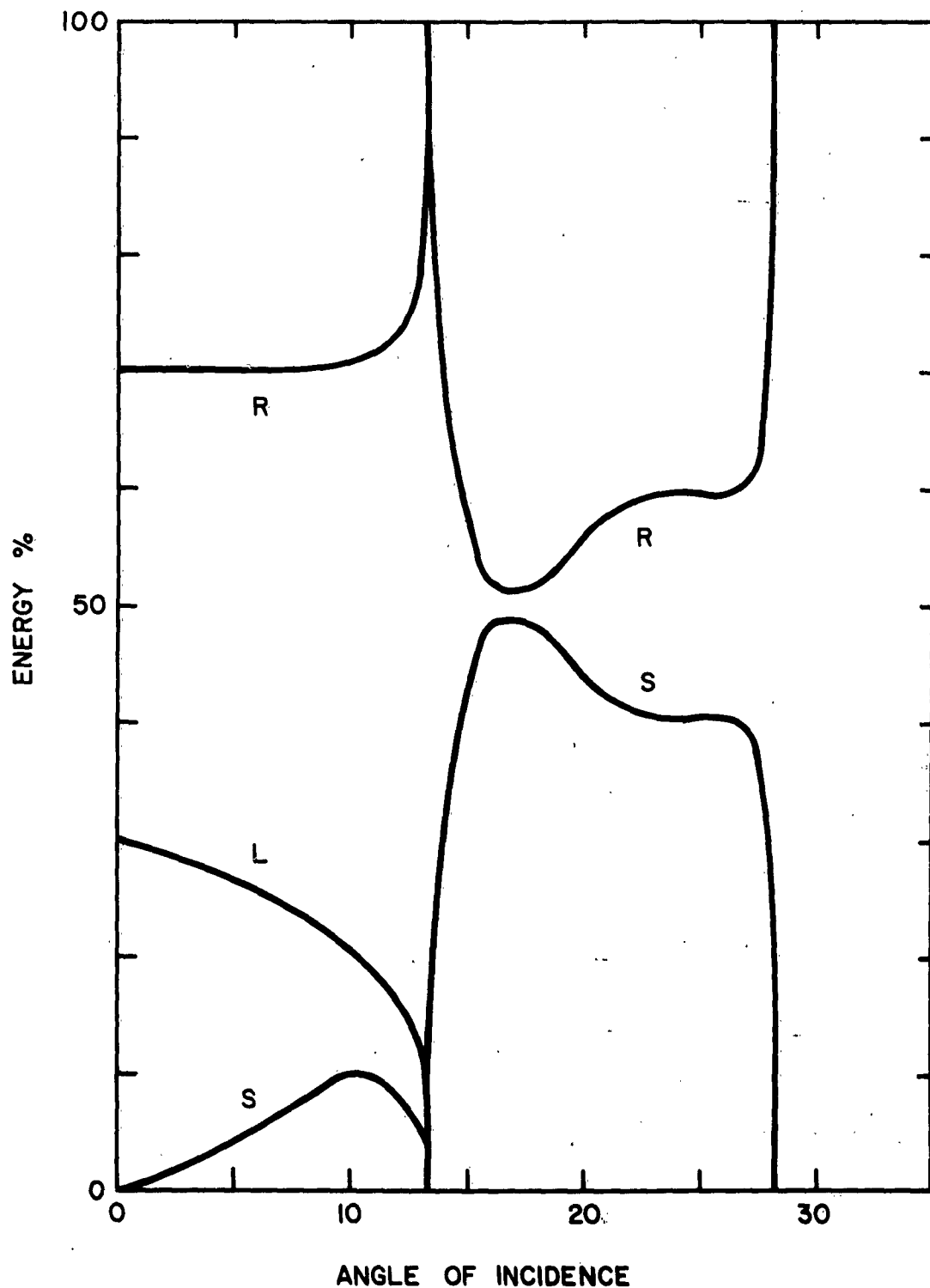


Figure 2 - Theoretical Energy Partition for a Water-Aluminum Boundary
(After Mayer (Ref. 5))

The relative sharpness of the (R) wave peak suggests that the angle corresponding to these peaks (or dips) might be determined with sufficient accuracy to monitor a variety of solid properties, particularly those near the surface. Furthermore, one might well consider the over-all curve of reflected energy versus angle of incidence as a sort of fingerprint that yields much information about the solid with a minimum amount of experimental difficulty. For example, such data could be obtained using frequencies that would be so highly attenuated in the solid itself as to prohibit more direct techniques.

If the possibility of surface wave generation is also considered at the liquid-solid boundary then the curves of Figure 2 would be modified somewhat. The major change will of course occur at angles of incidence beyond the angle, α_s , for critical refraction of the shear wave. At an angle just slightly greater than α_s the energy coupled into the surface wave will become a maximum and thus the reflected energy will dip again to another minimum.

Let us also consider a boundary that is somewhat more complicated than a simple liquid-solid interface. If the thickness dimension of the solid is of the same order of magnitude as the wavelength, or if the solid is made up of multiple layers having different properties, then the energy partition at the surface may be quite different than the example of Figure 2. This variation is due to flexural waves that may be generated either in free thin sheets or in surface sheets and coatings applied to thicker substrate material. The most commonly known and analyzed type of flexural waves are those known as Lamb waves.

Extension research in Lamb waves, (Refs. 15 and 16) sound transmission through plates, (Refs. 17 and 18) and Rayleigh waves (Refs. 19 and 20) have preceded this program. The references just given cover only a small fraction of the past work in these areas which are all pertinent to the energy partition that occurs upon ultrasonic reflection at a liquid-solid interface when the angle of incidence is varied. Our initial interest was in simply developing a quick and accurate method for evaluating the energy partition in interaction experiments involving immersion techniques. The availability of an ultrasonic goniometer, described in a previous report, (Ref. 1) greatly facilitated this work. The relative ease and accuracy of performing experiments with this apparatus suggested an extension of the original work to include at least a preliminary investigation of coated or laminated structures. The experimental apparatus and some of the results are given in the following sections.

B. Experimental Apparatus

The basic apparatus used here to study energy partition has been the "ultrasonic goniometer" that was originally designed to study beam interaction in solids (Ref. 1). The specimen stage was modified, however, and an angle indicator was added. A schematic presentation of the apparatus is shown in Figure 3. The stage angle indicator is not included in the schematic but it has a vernier which can be read to one minute of arc. Transducer A and transducer B are both immersion type units and can be operated either as transmitter and/or receiver. Each transducer and the specimen stage rotate independently about a common axis. The specimen is positioned on the stage by clamping it tightly against the cross-hatched face plates which are an integral part of the stage. This step insures that a line segment of the specimen's front surface is coincident with the axis of rotation.

The two transducers are each initially aligned for maximum reflection at normal incidence to the specimen. During the subsequent measurements, transducer A is operated as the transmitter and its position is locked so that the other transducer and the stage angle are measured from this reference position. The desired angle of incidence is set with the stage vernier and transducer B, used as a receiver, is then rotated until maximum signal is achieved. The amplitude of the received pulse as measured on an oscilloscope can then be easily plotted against the angle of incidence. Signal attenuation in the immersion liquid (water) is normalized out by simply removing the specimen from the stage and rotating the receiver crystal until it is exactly opposite the transmitter. The amplitude obtained in this configuration represents a "100 per cent reflection" value with which the reflected amplitudes can be compared directly.

In the experiments performed thus far, the two transducers each have a fundamental frequency of 15 Mc. but they have been operated at the third harmonic frequency of 45 Mc. At this frequency the beam spread is very small and angular settings are fairly reproducible. An evaluation of the angular reproducibility can be achieved by setting the two transducers and then rotating the stage until maximum signal occurs. The stage vernier is then read. When this procedure is repeated the stage angle is found to be reproducible to within approximately 2 - 3 min. Another source of error, however, becomes effective when one monitors the reflected signal amplitude. Due to electronic fluctuations, width of the oscilloscope trace, etc., it is difficult to measure the pulse height of the reflected signal with an accuracy better than 1 per cent.

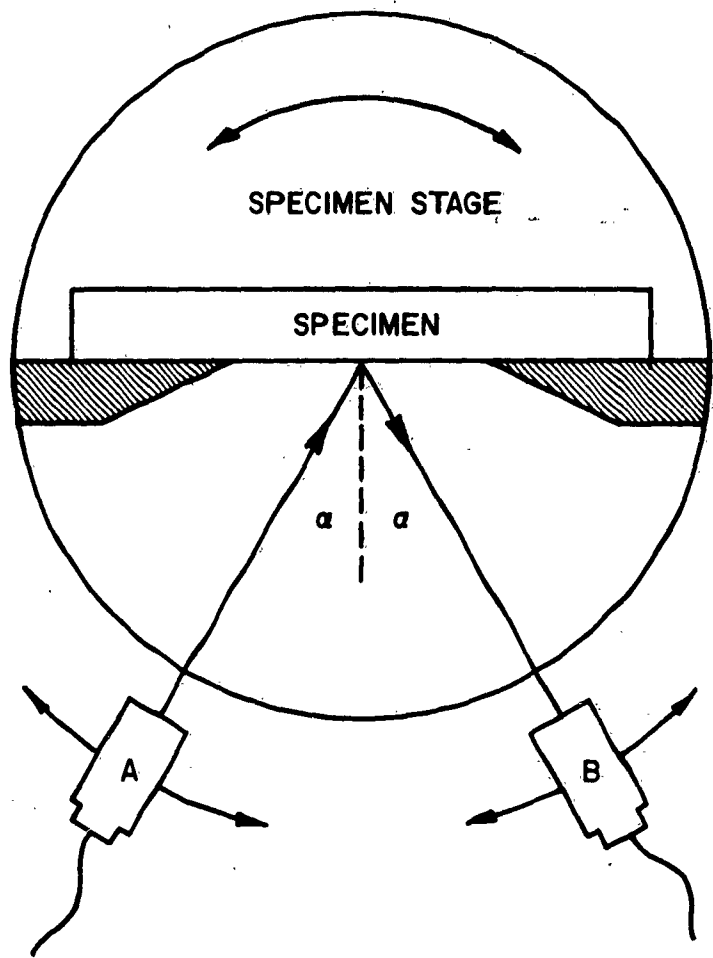


Figure 3 - Schematic of Apparatus for Studying Reflected Beam Amplitude versus Angle of Incidence, α

C. Results

Figure 4 is a plot of experimental data showing reflected energy versus angle of incidence for two different materials, 6061-T6 aluminum and 304 stainless steel. The curves start at approximately 12° because this is about as close together as we can get the two transducers with the present arrangement. The first part of the curve for aluminum is in excellent agreement with the theoretical curve of Mayer (see Figure 2). The peak labeled "A" occurs at an angle of incidence corresponding to a refraction angle of 90° for the longitudinal wave. It is particularly interesting to note that, in agreement with theory, height of this peak shows 100 per cent reflection indicating that none of the incident energy is going into a refracted shear wave. The position of the peak can, of course, be used to calculate the velocity of the longitudinal wave in aluminum. Since $\sin r = 1$, Snell's law reduces to the form,

$$v_2 = \frac{v_1}{\sin i} ,$$

where v_1 and v_2 are the longitudinal velocities in water and aluminum, respectively. Using $13^\circ 35'$ as the apparent angle of incidence corresponding to the peak position we calculated a longitudinal velocity for aluminum equal to 6,300 m/sec. This value is in very good agreement with 6,200 m/sec obtained in the same sample by pulse-echo techniques.

For larger angles of incidence the per cent of incident energy that is reflected drops away from the peak at A and reaches a minimum at B corresponding to the condition under which maximum energy is being refracted into the aluminum as a shear wave. The per cent energy reflected at this minimum again is in very good agreement with the theoretical curve of Figure 2. As the angle of incidence is increased further, the shear wave is critically reflected giving rise to the peak at C and then the curve dips to another minimum at D before climbing back to total reflection. The minimum at D corresponds to maximum conversion of the incident energy into surface waves.

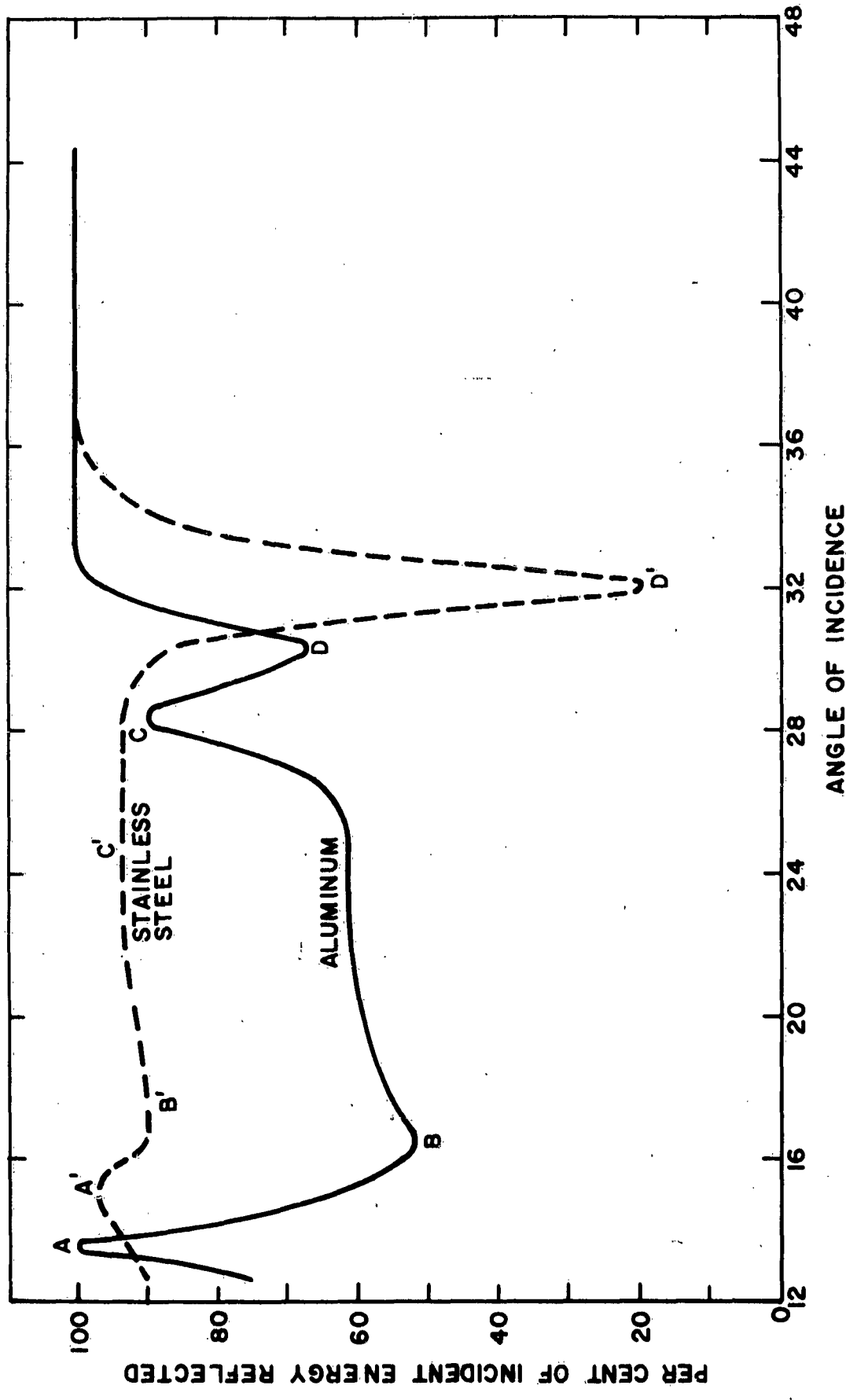


Figure 4 - Percentage of Incident Ultrasonic Energy that is Reflected versus the Angle of Incidence for 304 Stainless Steel and 6061-T6 Aluminum

The experimental data for stainless steel is similar to that of aluminum but, because of the greater impedance mismatch with water, more of the energy is reflected and the corresponding peaks and dips at A', B', and C' are of considerably smaller magnitude. The surprising characteristic of the stainless steel curve is the depth of the minimum at D'. These data suggest that, in spite of the severe impedance mismatch and the relatively high angle of incidence, approximately 80 per cent of the incident energy is converted into surface waves.

Let us now examine the reflected energy when thin films of pigmented acrylic resin are applied to the surface of 6061-T6 aluminum. The resin was sprayed onto the aluminum from a commercially available pressurized "spray paint" container. Figure 5 shows experimental curves for the bare aluminum substrate as well as several thicknesses of the resin. Amplitude of the reflected signal is shown here rather than the per cent energy. Furthermore, the height of each curve has been normalized to a common value at the first peak corresponding to critical refraction of longitudinal waves within the aluminum. We note that the angular position of this peak is essentially the same for all three curves. We interpret this as an indication that the films are still too thin to strongly influence the critical angle for longitudinal refraction. In other words, the aluminum substrate still controls the position of the peak. Beyond this peak, however, the curves are much less similar. It appears that the critical shear wave peak gets washed out and the "surface wave" minimum shifts to lower angles as thicker films are applied. This particular surface wave probably exists at the resin-aluminum interface. The sound velocities in the resin are so low that one would expect the critical angles for this material to be rather large. Therefore, as thicker films are applied and the influence of the resin becomes greater the curves would take on more structure at angles beyond 32° , where bare aluminum is normally total reflecting. Figure 5 seems to confirm this line of reasoning; however, interpretation would be more definite if "thick-film" data were available where the substrate influence was completely removed.

In an attempt to more closely control the thickness and uniformity of the variable layer we switched to a different composite system - that of brass shim stock bonded to a lucite substrate. The brass shim stock was degreased and slightly etched before the bonding was attempted. The actual bonding was performed by lightly brushing the lucite surface with ethylene dichloride and then pressing the shim stock and lucite against a flat plate with a pressure of approximately 1,000 psi.

The relative amplitude of the reflected signal versus angle of incidence for thick samples of brass and lucite is plotted in Figure 6. One can compare the actual magnitude of these two curves if the height of the lucite curve is reduced by a factor of ten. As expected from impedance arguments the lucite reflects much less of the incident energy at all angles.

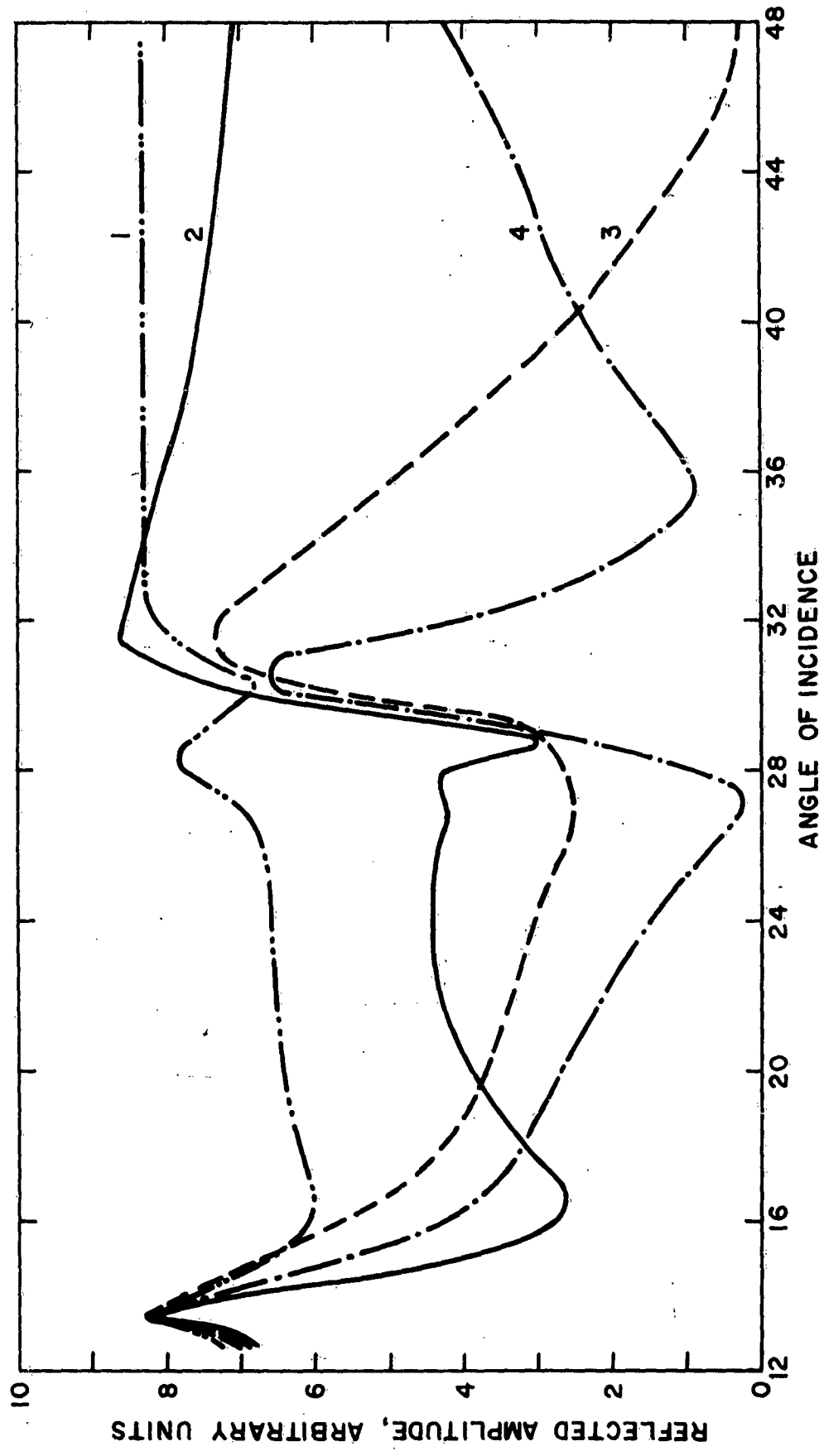


Figure 5 - Amplitude of Reflected Signal versus Angle of Incidence for (1) Bare Aluminum, and Aluminum Substrates Coated with Acrylic Resin Paint Having Thicknesses of (2) 0.0005 in., (3) 0.001 in., (4) 0.002 in.

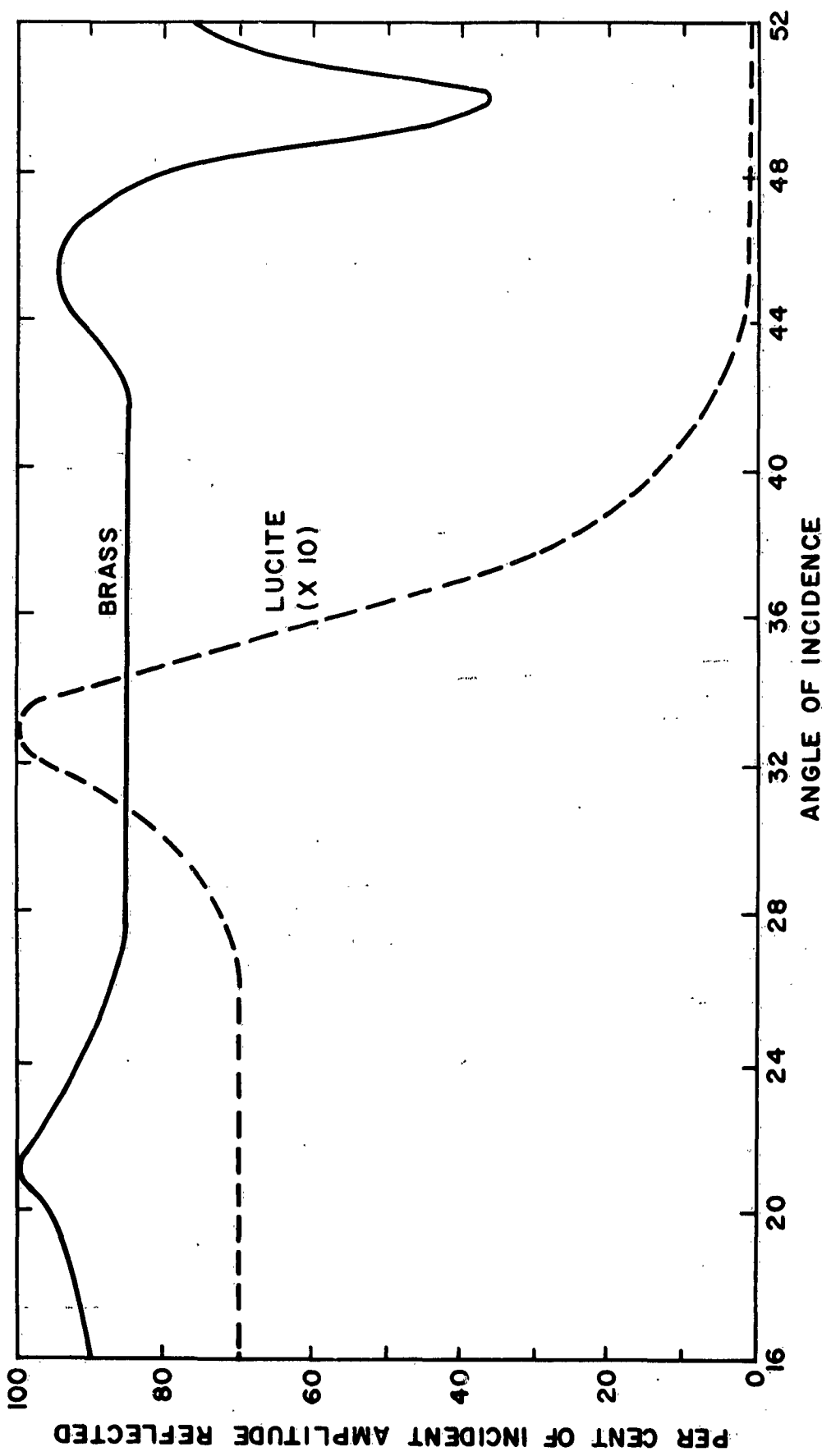


Figure 6 - Per Cent of Incident Amplitude versus Angle of Incidence for Brass and Lucite. To Compare the Two Curves, the Lucite Amplitudes Should be Reduced by a Factor of 10.

The curve for brass is very similar to that seen previously for aluminum except that the maxima and minima are all shifted toward larger angles in agreement with the lower velocities present in brass. Lucite, having even lower velocities, has a peak at 33° corresponding to critical longitudinal refraction and then the reflected energy falls off rapidly to almost zero. We did not investigate the situation at higher angles of incidence but one would not expect to find a "critical shear" maximum because the shear velocity is less than the longitudinal velocity in water. Thus, the angle of refraction for shear waves would be less than 90° for all angles of incidence.

Two typical curves for brass-lucite composites are shown in Figure 7. Neither of the curves resemble the plots of brass or lucite but some features are identifiable. It is interesting to note that the sample with the thicker brass (0.0042 in.) has a pronounced minimum at about 50° . This minimum was present and remained at approximately 50° for all samples in which the brass was thicker than about 0.003 in. All other details of the curves varied with thickness. The 0.003 in. dimension is approximately equal to the wavelength dimension for surface waves in brass at the frequency of our experiments. Thus, the surface wave minimum is seen to shift drastically (or vanish) for surface films less than approximately one wavelength thick.

The other maxima and minima of Figure 7 did not yield to immediate interpretation. Since the impedance mismatch between brass and lucite is so great, it was felt that the brass might be acting essentially as a free plate and the reflection minima would correspond to energy removed by Lamb waves. To check out the influence of the lucite substrate on these reflection measurements we subsequently obtained amplitude versus angle of incidence data for the same piece of shim stock first bonded to lucite and then bounded on both sides by water. The results were essentially identical indicating that the experiments of brass on lucite should be amenable to Lamb wave treatment. However, using the tables for brass given by Wrolton (Ref. 16), we calculated the angular positions which should excite the various Lamb wave modes and obtained rather poor agreement with our experimental results. The disagreement may be due to variations between the brass used by us and that used by Wrolton or it may be due to interference effects between the reflected signal and signals reradiated by the Lamb waves. Further work is necessary to completely clarify this point.

Another system that was examined briefly using the reflected energy technique was that of copper electroplated onto a substrate of stainless steel. With this system the impedance mismatch is not so severe as in the brass-lucite system and therefore one would expect the substrate to more strongly influence the experimental results. Figure 8 shows curves for bare stainless, bare copper, and stainless covered with an 0.0005 in. layer of copper. The surface wave minimum occurs at approximately 32° for stainless steel and about 46° for copper. A copper layer only one-half mil thick produced a shift in the position of this minimum to about 35° .

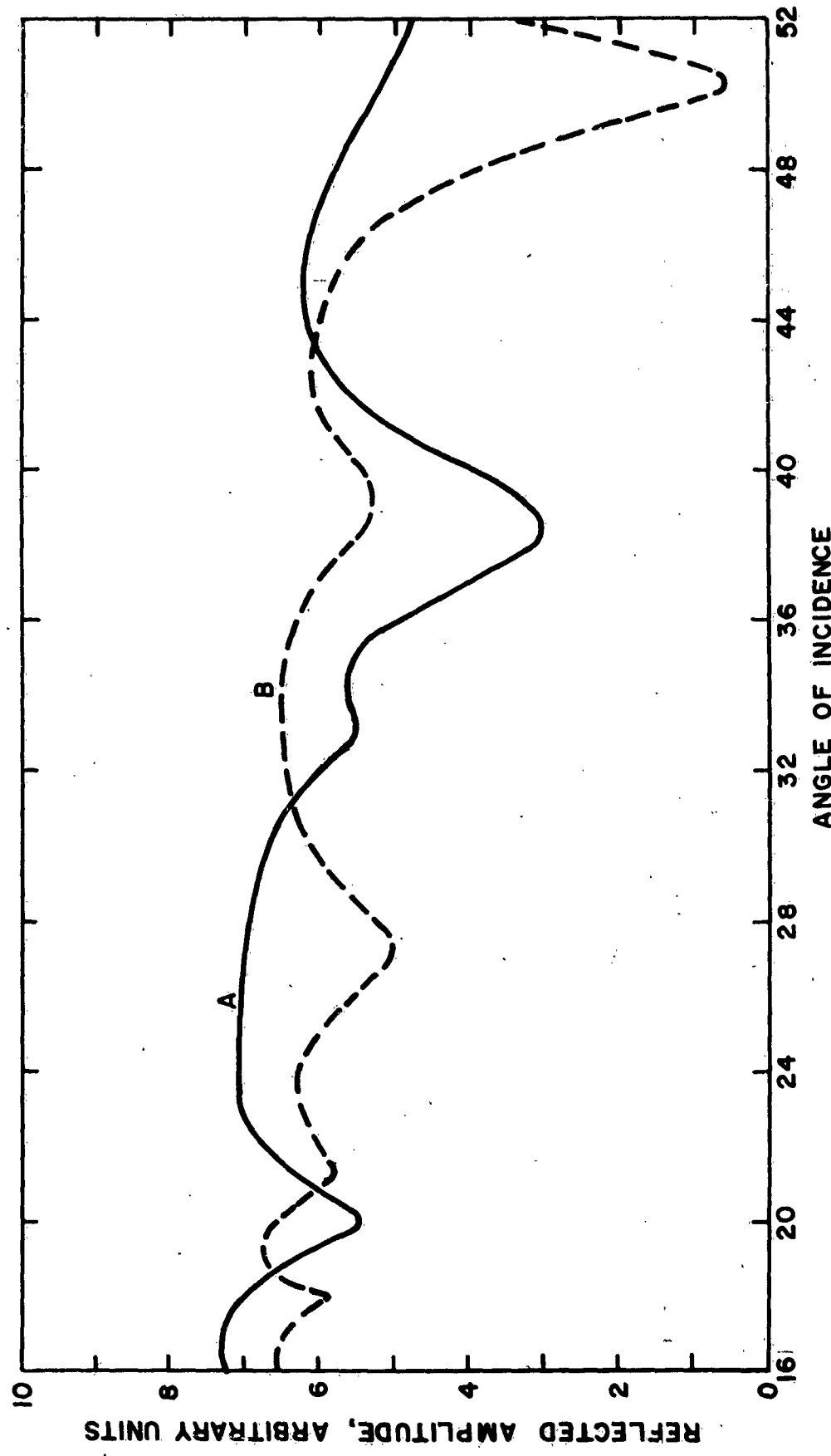


Figure 7 - Amplitude of Reflected Signal versus Angle of Incidence for (a) 0.002 in. Thick Brass on Lucite, and (b) 0.0042 in. Thick Brass on Lucite

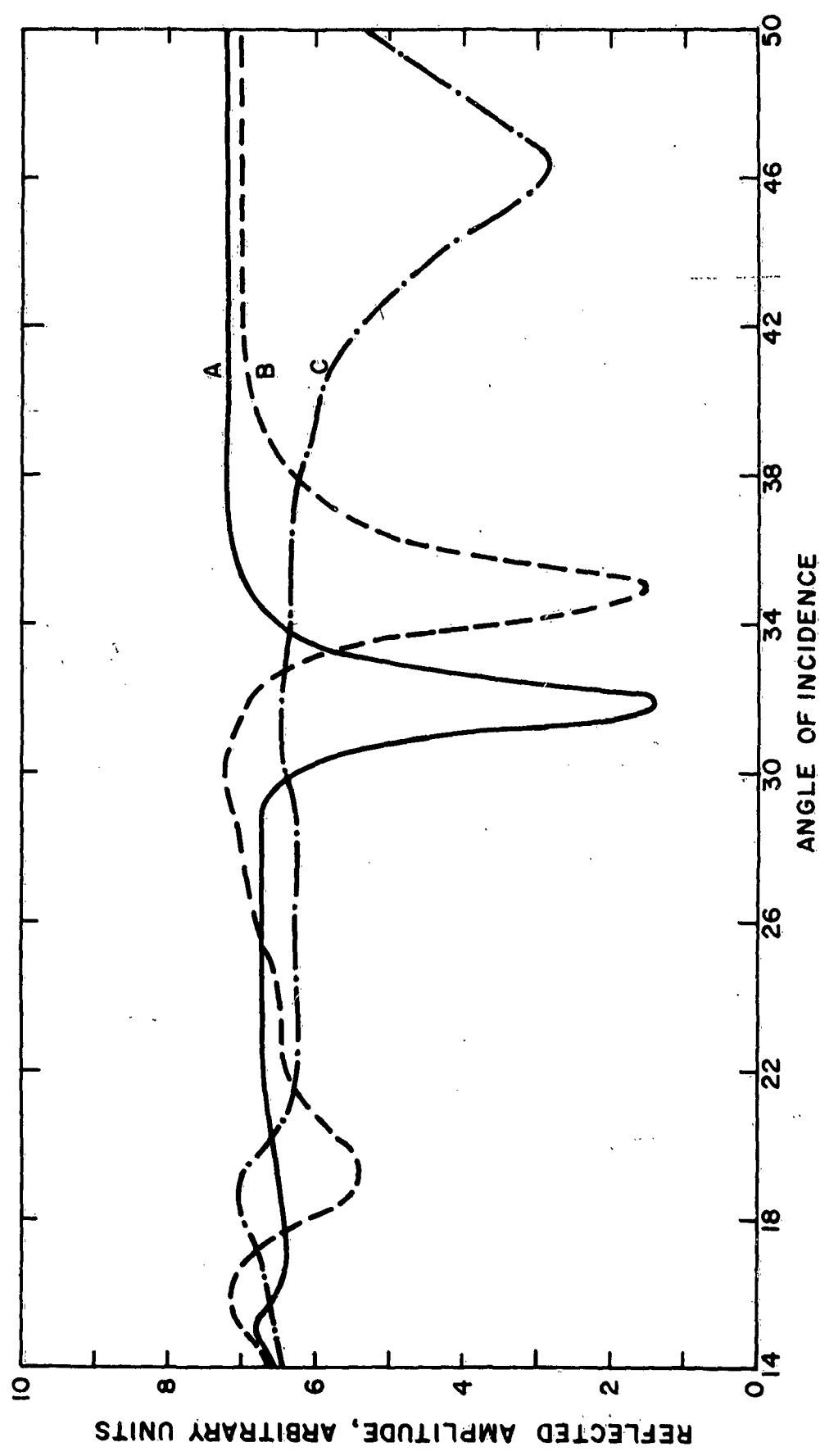


Figure 8 - Experimental Curves for (a) 304 Stainless Steel, (b) Stainless Steel with 1/2 Mil Thick Electroplated Copper, and (c) Copper

For thicker copper films the surface wave minimum continued to move to higher angles until it reached 46°, the angular position for surface wave generation in thick copper. Using the copper-stainless system we were able to observe effects caused by poor bonding between the two metals, but insufficient time was available to fully explore these effects.

The main conclusion to be drawn from the foregoing discussion is that an improved model of the ultrasonic goniometer would be a fast and valuable means of evaluating a multitude of surface characteristics, particularly where surface coatings of various types are involved. Such an instrument could be motor driven with a half-angle gearing arrangement whereby the detection angle of the receiving transducer would always equal the angle of incidence. The amplitude of the received pulse could in fact be automatically recorded against the angle of incidence very much like an x-ray automatic recording spectrometer. Such a device would not be very appropriate for complete scanning of large surface areas because of the time required. However, it could provide valuable information during spot check quality control or preventative maintenance operations. Furthermore, a plot of the reflected signal versus angle of incidence would facilitate the selection of optimum conditions for a high sensitivity, fast scanning test that could cover the surface if necessary. Many of the maxima and minima encountered as the angle of incidence is varied are extremely sharp. Some are very dependent on thickness while others are more strongly influenced by elastic properties of the surface or unbond between coating and substrate. A recording goniometer would permit a fairly rapid determination of the over-all surface characteristics of a particular system. This information could then be used to pinpoint the most sensitive test for the parameters or defects of major interest.

V. PAPERS, PUBLICATIONS, AND MEETINGS

During the past year, the following activities were directly related to work performed on this program: Mr. Rollins presented invited papers at the American Physical Society meeting in March and at the Symposium on Physics and Nondestructive Testing in September. The latter paper will be published as part of the Symposium Proceedings. In addition, Messrs. Rollins, Taylor, and Todd wrote two papers that have been published in the Physical Review (Refs. 3 and 4).

REFERENCES

1. Rollins, F. R., Jr., and L. Taylor, Tech. Documentary Report No. ML-TDR-64-21, Part I (1964).
2. Jones, G. L., and D. R. Kobett, Jour. Acoust. Soc. Amer., 35, 5 (1963).
3. Taylor, L., and F. R. Rollins, Jr., Phys. Rev., 136A, 591 (1964).
4. Rollins, F. R., Jr., L. Taylor, and P. Todd, Phys. Rev., 136A, 597 (1964).
5. Childress, J. D., and C. G. Hambrick, Phys. Rev., 136, A411 (1964).
6. Alers, G. A., and P. A. Fleury, Jour. Acoust. Soc. Amer., 36, 1297 (1964).
7. Heuter, T. F., and R. H. Bott, Sonics, John Wiley and Sons, p. 29 (1955).
8. Smith, R. T., Ultrasonics, 1, 135 (1963).
9. Rollins, F. R., Jr., Bull. Amer. Phys. Soc., 2, 117 (1963).
10. Rollins, F. R., Jr., Applied Physics Letters, 2, 147 (1963).
11. Rollins, F. R., Jr., WADD TR 61-42, Part I (1961).
12. Rollins, F. R., Jr., D. R. Kobett, and G. L. Jones, WADD TR 61-42, Part II (1962).
13. Mayer, W. G., J. Applied Physics, 34, 919 (1963).
14. Mayer, W. G., and C. E. Fitch, Jr., Papers presented at the 1964 Symposium on Physics and Nondestructive Testing, proceedings to be published.
15. Worlton, D. C., Nondestructive Testing, 15, 218 (1957).
16. Worlton, D. C., Lamb Waves at Ultrasonic Frequencies, HW-60662 Hanford Atomic Products Operation, Richland, Washington (1959).
17. Thurston, G. B., and A. Stern, A Bibliography on Propagation of Sound through Plates, Willow Run Labs., University of Michigan, Ann Arbor, Michigan (1959). Office of Naval Research, Contract Nonr-1224(24).

18. Fay, R. D., and O. Fortier, J. Acoust. Soc. Am., 23, 339 (1951).
19. Stonely, R., Monthly Notes Royal Astr. Soc., Geophys. Suppl., 6, (1954).
20. Firestone, F. A., and J. R. Frederick, J. Acoust. Soc. Am., 18, 2 (1946).